

**GOME-2
formaldehyde
retrieval sensitivity**

W. Hewson et al.

Characterisation of GOME-2 formaldehyde retrieval sensitivity

W. Hewson¹, H. Bösch¹, M. P. Barkley¹, and I. De Smedt²

¹EOS Group, Department of Physics and Astronomy, University of Leicester, Leicester, UK

²Belgian Institute for Space Aeronomy (BIRA-IASB), Avenue Circulaire, 3, 1180, Brussels, Belgium

Received: 30 August 2012 – Accepted: 11 September 2012 – Published: 24 September 2012

Correspondence to: H. Bösch (hb100@le.ac.uk)

Published by Copernicus Publications on behalf of the European Geosciences Union.

Title Page

Abstract

Introduction

Conclusions

References

Tables

Figures

⏪

⏩

◀

▶

Back

Close

Full Screen / Esc

Printer-friendly Version

Interactive Discussion



Abstract

Formaldehyde (HCHO) is an important tracer of tropospheric photochemistry, whose slant column abundance can be retrieved from satellite measurements of solar backscattered UV radiation, using differential absorption retrieval techniques. In this work a spectral fitting sensitivity analysis is conducted on HCHO slant columns retrieved from the Global Ozone Monitoring Experiment 2 (GOME-2) instrument. Despite quite different spectral fitting approaches, the retrieved HCHO slant columns have geographic distributions that generally match expected HCHO sources, though the slant column magnitudes and corresponding uncertainties are particularly sensitive to the retrieval set-up. The choice of spectral fitting window, polynomial order, I_0 correction, and inclusion of minor absorbers tend to have the largest impact on the fit residuals. However, application of a reference sector correction using observations over the remote Pacific Ocean, is shown to largely homogenise the resulting HCHO vertical columns, thereby largely reducing any systematic erroneous spectral fitting.

1 Introduction

Formaldehyde (HCHO) is an important atmospheric trace gas found throughout the troposphere, produced from the oxidation of volatile organic compounds. Methane oxidation is by far the biggest source of HCHO, sustaining global background levels (Stavrakou et al., 2009b). However, over continental regions large HCHO enhancements often occur to more localised VOC sources, and from HCHO directly released or produced from biomass burning or industrial processes; direct HCHO emissions from vegetation are a minor source. Since HCHO has a short atmospheric lifetime of only a few hours against photolysis and reaction with the hydroxyl radical (OH), it is a suitable proxy for detecting active photochemistry and determining surface VOC emissions (e.g. Palmer et al., 2003; Barkley et al., 2009; Stavrakou et al., 2009b; Curci et al., 2010; De Smedt et al., 2010; Boeke et al., 2011; Gonzi et al., 2011). In particular,

AMTD

5, 7095–7139, 2012

GOME-2 formaldehyde retrieval sensitivity

W. Hewson et al.

Title Page

Abstract

Introduction

Conclusions

References

Tables

Figures

◀

▶

◀

▶

Back

Close

Full Screen / Esc

Printer-friendly Version

Interactive Discussion



many studies have used satellite HCHO column observations to infer top-down emissions estimates of isoprene, which is the dominant biogenic VOC emitted from terrestrial vegetation (see Abbot et al., 2003; Palmer et al., 2003, 2006; Shim et al., 2005; Millet et al., 2006, 2008; Fu et al., 2007; Barkley et al., 2008; Stavrou et al., 2009a; Marais et al., 2012).

Despite HCHO's relatively high atmospheric abundance, its detection remains inherently difficult, due to its extremely weak absorption signature. Nevertheless, spaceborne monitoring of HCHO was first realised with the launch of the Global Ozone Monitoring Experiment (GOME) in 1995 (Burrows et al., 1999b), with Eisinger et al. (1997) and Thomas et al. (1998) publishing the first HCHO observations of a biomass burning event over Indonesia in 1997. Later work with the GOME dataset by Chance et al. (2000), incorporated major advances in the detection of minor absorbers, reducing fitting residuals on the HCHO slant column fit to around 5×10^{-4} , with fitting precision of $< 0.4 \times 10^{16}$ molecules cm^{-2} . Further retrievals by Wittrock (2006) and De Smedt et al. (2008), using spectral measurements from SCIAMACHY on-board ENVISAT, retrieved HCHO to a precision of about 1.0×10^{16} molecules cm^{-2} for a single observation. The larger fitting uncertainty of SCIAMACHY, compared with GOME, is attributed to its' finer spatial resolution, engendering a reduced signal to noise ratio (De Smedt et al., 2008). HCHO columns have also been observed from Ozone Monitoring Instrument (OMI), a CCD spectrometer aboard NASA's Terra satellite (launched 2004), through a non-linear direct fitting of radiances developed by Chance (2002) and Kurosu et al. (2004); reported OMI slant column uncertainties are about 40–100%. GOME-2, the successor to the original GOME mission, was launched in October 2006, with the initial retrievals of De Smedt et al. (2009, 2012) and Vrekoussis et al. (2010) yielding fitting precisions of $\sim 0.8 \times 10^{16}$ molecules cm^{-2} , and spatial distributions consistent with previous sensors.

However, despite a heritage of HCHO monitoring from space, the HCHO column retrievals still remain less well characterised when compared to major absorbers such as ozone (e.g. Van Roozendaal et al., 2002; Balis et al., 2008; Loyola et al., 2011b) and

GOME-2 formaldehyde retrieval sensitivity

W. Hewson et al.

Title Page

Abstract

Introduction

Conclusions

References

Tables

Figures

◀

▶

◀

▶

Back

Close

Full Screen / Esc

Printer-friendly Version

Interactive Discussion



nitrogen dioxide (e.g. Boersma et al., 2004; Richter et al., 2011; Valks et al., 2011). This work attempts to address this issue by presenting a detailed assessment and characterisation of GOME-2 HCHO retrieval uncertainties. Increased accuracy of the HCHO column product improves confidence in its use for constraining surface emissions.

2 Instrument and retrieval methods

The GOME-2 UV spectrometer is mounted onboard EUMETSAT's METOP-A spacecraft. Operating in a sun synchronous near-polar orbit, the satellite orbits the Earth every 101 min, with a local Equator crossing time of 09:30. GOME-2 samples the 240–790 nm spectral range with a spectral resolution between 0.24–0.5 nm, and a typical spatial resolution of $80 \times 40 \text{ km}^2$. GOME-2 minor absorber products are retrieved operationally by the GOME Data Processor using the standard differential optical absorption spectroscopy (DOAS) method (Loyola et al., 2011a). For HCHO, this involves fitting trace gas absorption cross sections to measured atmospheric absorption spectra; retrieving the HCHO slant column abundance along the instrument's viewing geometry. Slant columns are then converted to vertical columns, after division by an air mass factor computed using a radiative transfer model based on an assumed/known atmospheric and surface properties (Palmer et al., 2001; Martin et al., 2002).

In the analyses that follow, a default reference retrieval described in Table 1, is adjusted one setting at a time to determine the sensitivity of the DOAS retrieval within a range of optimised settings. Sensitivity is analysed with reference to the retrieved HCHO column, 1σ standard deviation of the HCHO column, and root mean square (RMS) of the residual for each fit. RMS residual is defined as the remaining spectrum following fitting of the modelled spectrum x^{fit} to our measured Earthshine spectrum x^{meas} , over a quantity n of detector pixels i within the wavelength range for which the DOAS analysis is performed:

GOME-2 formaldehyde retrieval sensitivity

W. Hewson et al.

Title Page

Abstract

Introduction

Conclusions

References

Tables

Figures

◀

▶

◀

▶

Back

Close

Full Screen / Esc

Printer-friendly Version

Interactive Discussion



$$\text{RMS} = \sqrt{\frac{\sum_i (x_i^{\text{meas}} - x_i^{\text{fit}})^2}{n}}. \quad (1)$$

The chosen reference retrieval settings are largely based on the initial GOME-2 HCHO characterisation of De Smedt (2011). By analysing the ensuing parameters with respect to the reference retrieval, differences in slant columns are attributed to systematic effects imparted by each parameter adjustment. The random error component of the retrieval (or the noise in GOME-2 measured Earthshine spectra) is reduced by analysing a monthly mean rather than individual orbits.

The DOAS retrieval itself is performed using the QDOAS analysis software (Fayt et al., 2011), prior to which, trace gas cross sections listed in Table 1 are corrected to vacuum wavelengths (where appropriate), and convolved with the GOME-2 slit function measured pre-launch (Siddans et al., 2006), using the daily Solar Mean Reference (SMR) wavelength grid taken from the relevant L1B orbit file. Ozone cross sections are corrected for the I_0 effect (Aliwell et al., 2002). Shift and stretch parameters are applied to Earthshine spectra, accounting for a very small error contribution from Doppler shift due to spacecraft and planetary motion. An improved wavelength calibration for the GOME-2 SMR I_0 reference is employed to further increase the accuracy of wavelength to pixel mapping, in order to further reduce fit residuals arising from mis-alignment of Earthshine and SMR spectra (Caspar and Chance, 1997; Van Geffen and Van Oss, 2003). Post-processing is initially limited to discarding observations with cloud fraction greater than 0.4 and solar zenith angles (SZA) of 60° . Monthly mean HCHO slant columns for August 2007, generated with this reference retrieval are shown in Fig. 1. An example DOAS fit for a region of enhanced isoprene emissions over the Southeast US (see Palmer et al., 2003), is presented in Fig. 2.

Global results are complemented by a detailed analysis for three $5^\circ \times 5^\circ$ sub-regions (detailed in Fig. 1), to examine regional effects potentially masked in the global statistic. The sites chosen reflect the range of HCHO column concentrations expected to be retrieved: (1) the remote Pacific (PAC) providing a clean reference in which only

GOME-2 formaldehyde retrieval sensitivity

W. Hewson et al.

Title Page

Abstract

Introduction

Conclusions

References

Tables

Figures

◀

▶

◀

▶

Back

Close

Full Screen / Esc

Printer-friendly Version

Interactive Discussion



background concentrations of HCHO are expected, (2) the South East United States (SEUS) at the height of the regional growing season, and (3) a portion of the Amazon rainforest (AMA) where large HCHO enhancements due to high biogenic emissions occur (Barkley et al., 2008). Results for all sites are given as means over their respective geographic area.

3 DOAS parameter sensitivities

Sensitivity test results are presented in Table 2, to which the reader is referred by test numbers inline and their corresponding descriptions. The sensitivity tests are divided into three groups: (1) spectral fit range, (2) spectral fit approaches, and (3) instrumental corrections. Following this, effects due to post-processing of slant columns are discussed in Sect. 4. Analysis of each setting accompanies the description of its influence on the retrieval.

3.1 Spectral fit range

Selection of an appropriate fitting window is known to be a major component of achieving an accurate DOAS fit, particularly for weak absorbers (Aliwell et al., 2002). Fit problems are prone to arise when different trace gas absorption features overlap, with weakly absorbing spectra (HCHO, BrO) masked by stronger absorbers (O_3 , Ring). HCHO is typically retrieved in the lower end of the UV between 325 and 360 nm (Witrock et al., 2000; De Smedt et al., 2008). A large degree of overlap between absorption cross sections is evident in this region, therefore the choice of fitting window immediately presents two problems which must be overcome to effect a reliable HCHO retrieval: (1) accurate retrieval of O_3 in the lower reaches of the fitting window, and (2) reduction of a false detection dichotomy between BrO and HCHO. Here a selection of fit windows relevant to the GOME-2 fitting range, and used throughout the literature, are tested.

GOME-2 formaldehyde retrieval sensitivity

W. Hewson et al.

Title Page

Abstract

Introduction

Conclusions

References

Tables

Figures

⏪

⏩

◀

▶

Back

Close

Full Screen / Esc

Printer-friendly Version

Interactive Discussion



3.1.1 BrO pre-fit

The pre-fitting technique has been used in GOME-1 and GOME-2 retrievals (Chance et al., 2000; De Smedt et al., 2012) to counter the effect of spectral similarities between BrO and HCHO. In the default test presented here, BrO is retrieved in a wide wavelength window (328.5–359 nm), using the same settings and spectra as found in the regular HCHO fit, with the exception of including scan bias correction spectra (EU-METSAT, 2011). Inclusion of these correction terms in both BrO and HCHO fit windows shows no discernible difference compared to scan correction in the BrO window alone, therefore in order to reduce the number of fitted parameters, corrections are applied to the BrO window only.

Based on the GOME-2 BrO retrievals as implemented in Theys et al. (2011), a slightly narrower BrO fit window is tested here in the 332–359 nm region, both with and without inclusion of the additional absorber OCIO (as implemented in Theys et al. (2011)'s original retrieval). In the first instance, test 1a adjusts the BrO fit window alone to give a 21 % increase in the global HCHO slant column mean, largely reflecting an increase in the slant columns of 0.06×10^{16} molecules cm^{-2} over oceans, with a negligible effect on fit residuals. Including OCIO in test 1b increases HCHO slant column means further (49 %) globally, with AMA showing a more pronounced increase than for 1a, although less so than the SEUS and PAC regions. Inclusion of OCIO in both BrO and HCHO fit windows is tested further on in the study, but it should be noted that fit residuals exhibit a tendency to decrease in parallel with additional fitting parameters. In the case of including OCIO here, whereby the additional absorber should be expected to be found only on regional scales at high latitudes during the polar springtime (Kühl et al., 2006), residuals are probably erroneously reduced.

Taking the pre-fitting concept further, Chance et al. (2000) have previously applied a three step pre-fitting procedure to GOME-1 data, fixing both BrO and O₃ in the HCHO window to pre-fitted values from preferential fitting windows. Test 1c applies this method with an O₃ pre-fit in the 325–335 nm window (using the basic O₃ retrieval settings from

AMTD

5, 7095–7139, 2012

GOME-2 formaldehyde retrieval sensitivity

W. Hewson et al.

Title Page

Abstract

Introduction

Conclusions

References

Tables

Figures

◀

▶

◀

▶

Back

Close

Full Screen / Esc

Printer-friendly Version

Interactive Discussion



Loyola et al., 2011a), along with the default BrO pre-fit detailed above. This two way pre-fit shows a slight but noticeable increase in HCHO slant columns and fit RMS, suggesting for GOME-2, the application of a further pre-fit is not worth the extra computation required.

Margins between differing BrO pre-fit windows are small, in terms of both retrieved HCHO slant columns, and fit residuals. Given the slightly higher HCHO slant columns and very small reductions in RMS found with test 1a, adjusting the pre-fit window to the new range may well appear justified, in line with Theys et al. (2011) findings of an improved BrO fit in this region.

3.1.2 HCHO

Shown in Fig. 3, the dependence of retrieved slant column and its error on the chosen fit window is demonstrated by repeatedly performing a DOAS fit on a single pixel (covering a region of strong HCHO emissions), incrementally adjusting the upper and lower fit window limits with a 0.5 nm step. The lowest band of fit residuals is found with a lower fit range between 328 and 329 nm, coinciding with the second major HCHO absorption peak, whilst slant column error serve to provide an estimate of the upper window cut off, displaying a band of error minima in the 345–349 nm region.

In test 2a we retrieve in the 325.5–350 nm fit range used by Marbach et al. (2010), taking in the strongest HCHO absorption peak available (326 nm) in the UV, as well as an extra BrO peak towards the visible. Whilst fitting in this region is seen to substantially increase HCHO slant columns ($+0.57 \times 10^{16}$ molecules cm^{-2} globally), fitting residuals similarly increase between $0.53\text{--}0.92 \times 10^{-4}$, pointing towards significant amounts of spectral interference from the wider band of strong O_3 absorption in the lower UV. A newly proposed fit region, 332–350 nm is tested for test 2b, with the intention of avoiding the worst O_3 absorption in the lower fit range. This sees a global reduction on HCHO slant columns of 27 %, along with noticeable increases in fit residuals (6 % globally), suggesting removal of the HCHO absorption peak around 330 nm imparts

GOME-2 formaldehyde retrieval sensitivity

W. Hewson et al.

Title Page

Abstract

Introduction

Conclusions

References

Tables

Figures

◀

▶

◀

▶

Back

Close

Full Screen / Esc

Printer-friendly Version

Interactive Discussion



a significant negative effect on retrievals, providing and insufficient number of peaks with which to accurately discriminate HCHO from its conflicting absorbers.

Testing similar space-borne UV spectrometer retrieval windows on GOME-2 data shows the trend in slant column reduction continues as we move to the lower end of the window further from the UV. In 2c we test the 337.5–359 nm fit window refined for use with the original GOME instrument (Chance et al., 2000; Wittrock et al., 2000). With the fit window lower limit at 337.5 nm, correlations between HCHO and O₃ spectra should be minimised in the DOAS fit – moving into a region of greatly reduced O₃ strength compared to the HCHO absorption spectra. However, reduction in the O₃ correlation comes at the cost of a greatly increased fitting residual (22 % globally), and major reductions in HCHO slant columns (-1.18×10^{16} molecules cm⁻²), due to increased interference from BrO and O₄. The comparable OMI sensor also provides spectra for HCHO column retrievals using a GOME type spectral fitting algorithm (Chance, 2002; Kurosu et al., 2004). Test 2d applies the suggested OMI retrieval window (327.5–356.6 nm) on the GOME-2 data (in conjunction with the standard BrO pre-fit), leading to enhanced retrieval residuals of approximately 10% compared to the reference retrieval, whilst we observe continental HCHO slant column decreases of 14–26 %.

From tests 2a–d, it is apparent that the differences between various spectrometers limit applications of fit windows as specific to each instrument. Possible sensitivity to the O₄ absorption cross section precludes use of the original GOME and OMI HCHO fit windows, due to their use of a higher wavelength cut off. Nevertheless, a good retrieval is possible with the lower fitting range as applied in the reference fit, with Fig. 3 demonstrating a minimisation of fit RMS is achieved, coupled to strongly enhanced HCHO slant columns expected of the SEUS study site.

GOME-2 formaldehyde retrieval sensitivity

W. Hewson et al.

Title Page

Abstract

Introduction

Conclusions

References

Tables

Figures

◀

▶

◀

▶

Back

Close

Full Screen / Esc

Printer-friendly Version

Interactive Discussion



3.2 Absorber effects

3.2.1 Ring effect

Modelling of the Ring effect is accounted for with the inclusion of Ring spectra as pseudo-absorbers in the retrieval. In the reference retrieval, the method of Vountas et al. (1998) is applied to Ring cross sections generated with the SCIATRAN radiative transfer model (Rozanov et al., 2005), accounting for both Fraunhofer and molecular Ring effects. The widely used alternative method of Chance (1998) applies only one pseudo-absorber in the retrieval, assuming the molecular contribution to Ring effect can safely be ignored. However, direct comparison with the Vountas et al. (1998) Ring method used in the reference retrieval is not possible, due to use of a slightly different slit function for convolution of the Chance (1998) Ring cross section, hence the result's exclusion from Table 2. Our Chance (1998) Ring is generated with the QDOAS analysis software; deriving a Gaussian slit function using a non-linear least squares fitting procedure, with a FWHM of 0.27 nm appropriate to the GOME-2 spectral resolution in the 335 nm region. The QDOAS fitted slit function is found to differ from the Siddans et al. (2006) measured wavelength dependent slit function, consistent with known post-launch fluctuations in GOME-2's slit function (Cai et al., 2012).

Results with the single Ring cross section show large reductions in HCHO slant columns ($\sim 20\%$), coincident with increases in fitting residuals ($\sim 10\%$), this is likely effected by a poorer fit of the Ring component in the retrieval, but must be interpreted with caution due to the differing slit functions used. Further reductions in fitting residuals can be expected with an improved Ring term, taking into account scene specific parameters on albedo, aerosol loading, and clouds. However, given the range of variables involved in this process, this is considered beyond the scope of this study.

GOME-2 formaldehyde retrieval sensitivity

W. Hewson et al.

Title Page

Abstract

Introduction

Conclusions

References

Tables

Figures



Back

Close

Full Screen / Esc

Printer-friendly Version

Interactive Discussion



3.2.2 O₄ inclusion

When using a narrow window from 328.5–346 nm, the reference HCHO window upper limit correlates well with an O₄ absorption minima, which when combined with application of a 5th order polynomial, should negate significant O₄ interference in this region (De Smedt et al., 2008). Testing the inclusion of O₄ shows a decrease in global fitting RMS, corresponding to a minor increase of HCHO slant columns. The possibility of an O₄ incursion in the upper fitting region, where O₄ absorption is strongest, has been explored by De Smedt et al. (2008), and substantiated by the results of tests 2c and 2d here – finding the HCHO slant column significantly drops off as the fit window upper limit is increased from 356.6 nm (2d) to 359 nm (2c). This is further tested in 3b, retrieving in the highest fit range of 337.5–359 nm (original GOME-1 window), with O₄ as a fitted absorber. Addition of the O₄ cross section does not appear to remedy the extremely low HCHO slant columns retrieved in test 2c for a higher upper fit window limit, with a broadly similar range of values obtained. These results combine to suggest retrievals making using of higher fitting windows (above 350 nm) are substantially affected by unquantified fitting interference with O₄, thereby reducing confidence in the depressed fit residuals found with inclusion of O₄ in narrower fit ranges such as the reference retrieval. Until further work is conducted to characterise this interference, the addition of an O₄ cross section in the HCHO fit is not recommended.

3.2.3 OCIO inclusion

Including OCIO in both fit windows is seen to affect HCHO slant columns less substantially than with O₄, where slight decreases in fit residuals are displayed (alluded to from its inclusion in BrO pre-fit window tests), concurrent with a global reduction in HCHO slant columns of approximately a third. However, OCIO's presence is inhomogenous over the globe, being largely confined to stratospheric polar regions, and active during polar springtime (Oetjen et al., 2011). By discarding scans with SZA > 60°, OCIO should not present a problem for HCHO, elevated concentrations of which

GOME-2 formaldehyde retrieval sensitivity

W. Hewson et al.

Title Page

Abstract

Introduction

Conclusions

References

Tables

Figures



Back

Close

Full Screen / Esc

Printer-friendly Version

Interactive Discussion



are largely confined to mid-latitudinal tropical regions. However, due to similarities between HCHO and OCIO absorption cross sections, signal contamination cannot be completely ruled out. False OCIO detection in tropical tropospheric regions will lead to a reduction in HCHO columns, whilst an OCIO contaminated signal in poleward regions may well yield artificially enhanced HCHO values. Test 3d includes OCIO in the DOAS fit, yielding lower HCHO values over the Pacific Ocean (-0.16×10^{16} molecules cm^{-2}), together with slightly decreased slant columns for AMA and SEUS regions (-0.09 and 0.08×10^{16} molecules cm^{-2}) and a moderate global reduction in fit RMS (-0.04×10^{-4}).

3.2.4 Wavelength calibration

Although an extensive pre-flight characterisation campaign for the GOME-2 instrument (Siddans et al., 2006) has allowed for a superior operational wavelength calibration compared with its predecessor, additional wavelength calibration on reference spectra prior to application of DOAS fitting, is deemed essential. To test the usefulness of this extra calibration, the wavelength calibration step is omitted from the reference retrieval in test 3e. This results in a global reduction of HCHO slant columns by 0.81×10^{16} molecules cm^{-2} , coupled to an amplification in global latitudinal bias evident in the geographical distribution (see Fig. 4). Fit quality is reduced, with residuals deteriorating at a global scale (0.31×10^{-4}). This shows the improved wavelength calibration allows for an enhanced alignment of absorption features in spectra and trace gas cross sections, crucial in improving the accuracy of O_3 and BrO fits, particularly at high SZAs.

3.2.5 I_0 correction

Following the recommendation of Aliwell et al. (2002), O_3 cross sections included in the reference retrieval are corrected for the I_0 effect. The baseline retrieval followed here adds a concentration of 0.8×10^{19} molecules cm^{-2} back into the O_3 cross sections prior

GOME-2 formaldehyde retrieval sensitivity

W. Hewson et al.

Title Page

Abstract

Introduction

Conclusions

References

Tables

Figures

◀

▶

◀

▶

Back

Close

Full Screen / Esc

Printer-friendly Version

Interactive Discussion



to fitting (our reference retrieval shows O_3 retrieved in the slightly wider BrO pre-fitting window to be close enough to values retrieved in the HCHO window to warrant using the same correction value). The slant column amount to add back to the cross sections remains a source of error in the retrieval, typically set to the maximum retrieved slant column value of the corrected absorber. This value can be expected to exhibit wide seasonal and geographic variation. For orbit 4176, the scaling factor is adjusted in 0.1×10^{19} molecules cm^{-2} steps between 0.1 and 2.1×10^{19} molecules cm^{-2} to evaluate the range of retrieval effects imparted by the correction.

Figure 5 shows the results of this test, with a levelling off of HCHO slant columns and errors, O_3 and fit residuals when the column add back is increased above 0.5×10^{19} molecules cm^{-2} . Assuming the retrievals from orbit 4176 are reasonably illustrative of a typical GOME-2 orbit, this indicates an O_3 column add back of 0.5×10^{19} molecules cm^{-2} represents an appropriate correction factor. Extending the application of I_0 correction from just O_3 to all trace gas absorbers in test 3f yields negligible global increases in HCHO slant columns, with accompanying decreases in fit residuals of 0.04×10^{-4} . However, these changes are not uniform across the globe, with slant columns increasing for the AMA and PAC regions, and decreases evident for SEUS. These further reductions of fitting residuals suggests extending the I_0 correction methodology to all fitted trace gas absorbers to be warranted.

3.2.6 Cross section temperature

Change in absorption spectra line shape and strength are frequently encountered in parallel with temperature variations. Of relevance here, O_3 absorption cross sections show a strong relationship with both temperature and pressure (Liu et al., 2007), and are therefore included in the retrieval at two temperatures, orthogonalised to one another. Tropospheric HCHO retrievals typically fit O_3 at temperatures suitable to the stratospheric O_3 component, at around 218–228 K and 241–248 K.

GOME-2 formaldehyde retrieval sensitivity

W. Hewson et al.

Title Page

Abstract

Introduction

Conclusions

References

Tables

Figures

◀

▶

◀

▶

Back

Close

Full Screen / Esc

Printer-friendly Version

Interactive Discussion



**GOME-2
formaldehyde
retrieval sensitivity**

W. Hewson et al.

Title Page

Abstract

Introduction

Conclusions

References

Tables

Figures

◀

▶

◀

▶

Back

Close

Full Screen / Esc

Printer-friendly Version

Interactive Discussion



To test the dependence of HCHO slant column on O_3 retrieval temperature, we apply temperature coefficients given with the Liu et al. (2007) interpretation of the Malicet et al. (1995) O_3 cross sections, thus allowing accurate derivation of O_3 absorption cross sections at any number of temperatures. As shown in Fig. 6, the variability is assessed for a single scan over the SEUS study site, on the 9 August 2007 (scan no. 3107, orbit 4176), when a high HCHO slant column magnitude is expected. The O_3 temperature range is adjusted through 215–230 K and 235–250 K in 0.5 K intervals, altering retrieved HCHO slant columns between $4.25\text{--}4.5 \times 10^{16}$ molecules cm^{-2} , and O_3 slant column from $2.26\text{--}2.31 \times 10^{19}$ molecules cm^{-2} . Temperature effects on fit residuals are limited to a small range of O_3 temperatures between 220 K (lower) and 245 K (upper), beyond which, they flatten out around 7.11×10^{-4} . This large range of minimised fit residuals allows optimisation of the HCHO fit according to the maximum slant columns. For HCHO and O_3 , both suggest temperatures currently in use are entirely suitable (i.e. 228 and 243 K, respectively). Further increases may be found by adjusting the upper O_3 temperature beyond 248 K – with the possibility of fitting tropospheric O_3 .

The HCHO cross section varies throughout the UV absorption region (Brauers et al., 2007). To arrive at an appropriate error estimate for HCHO temperature dependency, HCHO cross sections were generated at 5 K temperature intervals between 273 and 308 K, and applied in place of the regular HCHO cross section (298 K). The mean temperature dependency over orbit 4176 is found to be weak, at only $\sim 0.03 \times 10^{16}$ molecules cm^{-2} over the 35 K temperature range tested, translating to an average decrease in HCHO slant column of 0.11 % per extra K.

Selecting two $5^\circ \times 5^\circ$ regions of high (South Eastern USA) and low (Gulf of Mexico) HCHO concentrations from the orbit provides a more detailed estimate of the temperature dependency. O_3 slant columns remain unaffected by the adjustment of HCHO absorption cross section temperature. Corresponding to the increased cross section temperature, HCHO slant column mean increases in a linear fashion $+0.16 \times 10^{16}$ molecules cm^{-2} across the temperature range for the the enhanced SEUS HCHO plume, with a much smaller increase for the low HCHO slant column

case, increasing by just 0.01×10^{16} molecules cm^{-2} . In both high and low HCHO cases, RMS varies within a negligible range on the order of $\times 10^{-7}$.

HCHO cross section temperature would ideally be selected appropriate to environmental conditions at the time of spectra recording. However, given the likelihood of information on tropospheric temperatures being available to the user, application of a mean tropospheric temperature for the entire orbit may represent the most practical solution. In this instance, for tropospheric mid-latitude HCHO retrievals, a temperature of 298 K would seem applicable.

3.3 Polynomial degree

Fitting the GOME-2 measured Earthshine spectrum with a polynomial removes the broadband spectral component of atmospheric Rayleigh and Mie scattering prior to fitting trace gas absorbers. Work with the original GOME instrument found application of a 3rd order polynomial sufficient to remove the atmospheric scattering component (Wittrock et al., 2000). However, with the reduction in width, and shift of the spectral range further into the UV, allowing stronger O_3 absorption to increase retrieval interference, a 5th order polynomial is applied in the reference settings, based on the work of De Smedt et al. (2012). Test 4a applies a fourth order polynomial, resulting in an approximate doubling of slant columns over oceans, with gains in HCHO SC of 24 % for AMA, and 44 % for SEUS. Application of a third order polynomial in test 4b increases the strength of the latitudinal dependency globally (reducing values at high latitudes, with increased slant columns at mid-latitudes), yielding a global HCHO slant column increase of around 15%. Fit residuals for both tests are seen to greatly increase (0.1×10^{-4} for the 4th order, and 0.3×10^{-4} for the 3rd globally) from the reference retrieval as we move away from the 5th order polynomial, showing lower order polynomials are unable to provide sufficient corrections for atmospheric scattering processes.

GOME-2 formaldehyde retrieval sensitivity

W. Hewson et al.

Title Page

Abstract

Introduction

Conclusions

References

Tables

Figures

◀

▶

◀

▶

Back

Close

Full Screen / Esc

Printer-friendly Version

Interactive Discussion



3.4 Instrument corrections

In a similar fashion to modelling atmospheric absorbers as accurately as possible presented in Sect. 3.2, mitigation must be made for known instrumental issues. In many cases this can be conducted by the addition of pseudo-absorbers representing spectral artefacts.

3.4.1 Scan bias

GOME-2 exhibits a scan angle and SZA dependent bias, occurring as a function of instrument degradation since launch (Cai et al., 2012). This is known to affect all GOME-2 retrievals, particularly those making use of the lower UV (Balis et al., 2008; Antón et al., 2009; Loyola et al., 2011b). To counter this scan bias, Eta and Zeta polarisation vectors (measured pre-launch) are included in the reference retrieval BrO pre-fit window as pseudo-absorbers. Visual inspection of individual orbits reveal the values retrieved for the Eta and Zeta parameters display distinctive east and west components. Confirmation of the corrective effect is made in test 5a by testing the retrieval without the vectors and examining individual swaths, allowing a strong cross track dependency to become apparent, highlighted by eastern slant columns retrieving between $1-2 \times 10^{16}$ molecules cm^{-2} higher than their western counterparts over clear ocean, manifesting in a globally increased HCHO slant column mean (0.4×10^{16} molecules cm^{-2}). However, exclusion of these correction factors also serves to significantly reduce fit residuals for all sites, with global reductions of 0.06×10^{-4} , and similar reductions of 0.05 and 0.04×10^{-4} for AMA and SEUS sites, respectively. This reduction in fit residuals points to the need for implementation of superior retrieval based bias correction techniques such as that derived by Loyola et al. (2011b), or empirical corrections of L1B data.

GOME-2 formaldehyde retrieval sensitivity

W. Hewson et al.

Title Page

Abstract

Introduction

Conclusions

References

Tables

Figures

◀

▶

◀

▶

Back

Close

Full Screen / Esc

Printer-friendly Version

Interactive Discussion



3.4.2 Spectral under-sampling

GOME-2 samples between 2.46 and 2.25 measurements per FWHM (0.27 nm) at the lower and upper wavelength limits of the reference fitting interval. Minute wavelength shifts of the spectrometer in orbit introduce potential for undersampling of spectra, especially with a moderately decreasing FWHM towards the upper limit of the HCHO fit window (Cai et al., 2012). Under-sampling spectra are calculated for GOME-2 following Chance et al. (2005), and included as a pseudo-absorber in the reference retrieval. Testing the efficacy of the under-sampling correction by excluding the spectra from the fit in test 5b, leads to a noticeable increase in global fit residuals (0.11×10^{-4}). Loss of retrieval sensitivity from not correcting for under-sampling, particularly for weak absorbers, suggests the inclusion of an under-sampling correction should be strongly considered.

3.4.3 Offset correction

A small amount of signal measured by GOME-2 is thought to be additive from extraneous sources inherent to the imperfect nature of the instrument's design, construction and operation (e.g. stray light in the spectrometer housing, and degassing of adhesives and materials). These predominantly systematic artefacts can be accounted for by the addition of a linear offset term in the DOAS fit – typically taking the form of fitting a 1st order polynomial to the fit residual (as used in the reference fit here). This is tested in comparison with a 0 and 2nd order offset polynomial (tests 5d and 5e), as well as application of a $1/I_0$ spectrum fitted as a pseudo-absorber (in place of the standard polynomial) (Marbach et al., 2010; Valks et al., 2011). The latter method, tested in 5f, has the potential to provide a more accurate representation of the offset term, being based on the instrument's physical parameters for each daily reference spectra.

Increasing the offset polynomial to a 2nd order correction reduces fit RMS (-0.04×10^{-4} globally), with corresponding increases in HCHO slant column for all sites ($\sim 0.06 \times 10^{16}$ molecules cm^{-2}), suggesting the correction offers a superior

GOME-2 formaldehyde retrieval sensitivity

W. Hewson et al.

Title Page

Abstract

Introduction

Conclusions

References

Tables

Figures

◀

▶

◀

▶

Back

Close

Full Screen / Esc

Printer-friendly Version

Interactive Discussion



modelling of instrumental offset. Application of a 0 order offset polynomial, and a $1/I_0$ spectrum as the offset term both show similar significant reductions in slant columns, with fitting residuals increasing beyond that found with the reference correction term - rendering both alternatives unsuitable for further application to the HCHO retrieval.

4 Sensitivity of HCHO vertical columns

4.1 Air mass factor calculation

GOME-2 HCHO vertical columns are obtained by dividing the slant columns from the optimised retrieval settings, with Air Mass Factor (AMF) values calculated offline using the approach of Palmer et al. (2001). As a full description of the AMF calculation is provided in Barkley et al. (2012a), we only provide a short-description. In brief, AMF look-up tables at 340 nm are constructed using the LIDORT radiative transfer model (Spurr et al., 2001), using monthly averaged HCHO profiles and aerosol optical depths, appropriate to GOME-2's overpass, from a global $4^\circ \times 5^\circ$ GEOS-Chem chemistry transport model simulation. A description of the GEOS-Chem simulation can be found in Barkley et al. (2012b). The monthly AMF look-up tables are parameterised as a function of solar zenith angle, viewing geometry, surface reflectance, and surface pressure. Partially cloudy pixels are accounted for with the independent pixel approximation method (Martin et al., 2002), with clouds treated as Lambertian reflectors with an albedo of 0.8. Cloud fraction and cloud-top pressure are taken directly from the GOME-2 GDP4.0 FRESCO product (Wang et al., 2008). The surface reflectance in clear-sky conditions is taken from the TOMS climatology of Herman and Celarier (1997). The AMF is known to be a significant source of uncertainty in the HCHO vertical column retrieval (De Smedt et al., 2008; Barkley et al., 2012a), and its impact on the GOME-2 retrieval will be examined in more detail in a future study.

GOME-2 formaldehyde retrieval sensitivity

W. Hewson et al.

Title Page

Abstract

Introduction

Conclusions

References

Tables

Figures

◀

▶

◀

▶

Back

Close

Full Screen / Esc

Printer-friendly Version

Interactive Discussion



4.2 Reference sector correction

To mitigate for unresolved spectral dependencies occurring at high latitudes between HCHO and strongly interfering BrO and O₃ molecules, a reference sector correction (RSC) is performed following the standard procedure developed for stratospheric correction of NO₂ retrievals (Martin et al., 2002; Richter and Burrows, 2002) and also routinely applied to HCHO data (e.g. Palmer et al., 2006; Barkley et al., 2008; De Smedt et al., 2008). A daily correction from a latitudinal reference strip of clean Pacific air between 140–160° W longitude is fitted with a 3rd order polynomial, and subtracted globally from each day's measurements. HCHO concentrations in this Pacific Ocean region are representative of global background levels generated by methane oxidation. Differences from this subtraction are attributed to unresolved spectral interferences and latitudinal dependency of the sub-optimal O₃ retrieval. Vertical columns are then derived by dividing bias free slant columns with previously generated AMFs. Finally, latitudinal means of GEOS-Chem model data (also fitted with a 3rd order polynomial over the same Pacific Ocean reference strip) are added back to generate the final corrected HCHO vertical columns.

A single GOME-2 scan packet contains 32 scans (assuming no post-processing filtering by SZA or CF), consisting of 24 high resolution front (forward sweep of instrument operation, measuring 80 × 40 km²) and 8 back scans (wide scans obtained in the rapid back sweep to the scan start position, measuring 240 × 40 km²). Here the front scans are further divided into east, centre and west components, consisting of 8 scans each, allowing investigation into the effect of the GOME-2 scan bias on the Reference Sector Method (RSM), and final vertical columns. Figure 8 and Table 3 show that by incorporating all scans into the correction, directional scan bias averages out over the swath, whilst including only east or west scans imparts a clear bias on the subtractive polynomial according to scan direction applied. Nevertheless, the scan bias correction remains essential, with error at swath edges likely to propagate through monthly and seasonal means.

GOME-2 formaldehyde retrieval sensitivity

W. Hewson et al.

Title Page

Abstract

Introduction

Conclusions

References

Tables

Figures



Back

Close

Full Screen / Esc

Printer-friendly Version

Interactive Discussion



4.3 Homogenisation of HCHO vertical columns

To test the effect of the application of the reference sector correction on the HCHO retrieval, differences in HCHO slant columns are compared with their corresponding vertical columns for all tests. Selected HCHO vertical column results are summarised in Table 4. This demonstrates major reductions in differences between test retrievals and the reference retrieval, particularly so for tests with previously very large differences, bringing all global vertical column differences within 21 % of the reference, compared to a maximum slant column difference of -390 %.

Despite widely varying errors in terms of fit residuals between retrievals, Table 5 demonstrates that application of the reference sector correction apparently causes previously disparate retrievals to converge around a broadly similar set of results. This ranges from those tests with small effects on global slant column mean (such as test 3f – I_0 correcting all absorbers, with previous slant column differences on the reference retrieval of 0.03 % converting to 1.69 % in vertical columns), to those with the largest effects (test 2c – fitting in the original GOME-1 HCHO retrieval window whose global slant column difference of -390 % is reduced to just -21 %). Of note, tests 2a, 2c, 4a and 5a stand out due to their extremely large slant column to vertical column differences. Based on the PAC study site, the vast majority of this variability can be attributed to retrievals at or around the limit of HCHO detection. Ocean retrievals typically return very low HCHO slant column values, with its production determined only by CH_4 oxidation rather than the spatially limited enhanced continental isoprene sources.

This homogenisation effect on the HCHO vertical columns occurs because once the slant column bias over the Pacific Ocean is subtracted, subsequent corrected slant columns are at or close to zero. Addition of a common GEOS-Chem model HCHO background therefore simply results in HCHO vertical columns of similar magnitude (irrespective of the spectral fitting procedure). However, whilst the reference sector method adjusts HCHO VCs to within similar orders of magnitude, it should be noted that the overall effect is to correct for a global offset, and latitudinal variation caused

AMTD

5, 7095–7139, 2012

GOME-2 formaldehyde retrieval sensitivity

W. Hewson et al.

Title Page

Abstract

Introduction

Conclusions

References

Tables

Figures

◀

▶

◀

▶

Back

Close

Full Screen / Esc

Printer-friendly Version

Interactive Discussion



by spectral interference with ancillary absorbers at high latitudes. By not discriminating spatially, the technique maintains compatibility and comparability between the various retrievals.

4.4 Cloud screen testing

5 As previously mentioned, scans with an effective cloud fraction of > 0.4 are initially excluded from analysis. Here the effect of increasing and decreasing the CF threshold for the reference retrieval is specifically examined. The high spatial resolution of GOME-2 should be able to tolerate the higher rejection rate on cloudy pixels for lower cloud fractions. This will yield a higher signal to noise ratio in monthly slant column means, 10 due to the reduction in slant columns whose fits are artificially adjusted due to cloud scattering and absorption effects.

Figure 9 shows the effect this cloud fraction adjustment has on the monthly HCHO slant columns and scan counts. A cloud fraction of 0.4, used as the reference threshold, is seen to offer a reasonable compromise between elimination of cloudy pixels without significantly affecting slant column values. However, comparison of slant columns with 15 vertical columns in Fig. 9 reveals that for the regions of enhanced HCHO, the statistic is affected by above cloud enhancements, resulting from the AMF taking a greater fraction of cloud albedo into account. This is further illustrated in Fig. 10, particularly for the AMA study site, where the majority of cloud can be seen to be sitting in the 20 300–600 hPa region.

Slant and vertical column statistics for the PAC region are stable above a cloud fraction limit of 0.1, whilst minor correlations between increasing scan counts and vertical columns are noted for the AMA region. This situation is mirrored, albeit with a lower intensity, for the SEUS region, whose slant and vertical column values increase sharply 25 in parallel with lower cloud fraction limits. Given the similarity in AMA and SEUS slant columns, the contrasting vertical column increase between the two regions likely results from subtle modulations in the AMF arising from widely differing cloud top pressures

GOME-2 formaldehyde retrieval sensitivity

W. Hewson et al.

Title Page

Abstract

Introduction

Conclusions

References

Tables

Figures



Back

Close

Full Screen / Esc

Printer-friendly Version

Interactive Discussion



(CTP) for specific cloud fractions between the regions, with dense, low cloud cover for the Amazon providing CTPs typically at the higher end of the scale.

5 Conclusions

This work presents an in-depth analysis of the parameters governing the accuracy and efficacy of GOME-2 DOAS HCHO retrievals. Testing has shown the major parameter influencing the minimisation of fitting residuals for HCHO fitting to be the spectral fit window, adjustment of which is shown to produce changes in retrieved slant column between 190 and -390% globally. Polynomial order, I_0 correction and fitted ancillary absorbers also have a significant impact on the fit residual. Smaller effects are found with instrumental correction, such as undersampling and offset correction, although these should be probably weighted with equal importance, since the HCHO retrieval is close to the limits of the instrument's sensitivity. Reference fit settings (Table 1) are found to provide an optimal group of parameters for global HCHO retrievals, based on the minimisation of error each setting is seen to provide in contrast to viable alternatives.

Vertical columns are much less sensitive to the input fitting parameters than their slant columns, primarily due to application of the RSM technique. Analysis has shown that regardless of spectral fitting parameters, which often result in large slant column differences, addition of model HCHO background columns to the bias corrected slant columns allows convergence of the final GOME-2 vertical column product to within a range of 16 to -21% globally for the various HCHO fitting windows. Cloud fraction is shown to have a large effect on both the monthly mean slant and vertical columns, the latter being affected by the relationship between the observed cloud top pressure and the HCHO vertical distribution.

Acknowledgements. This work was supported by the UK National Centre for Earth Observation (NCEO) and the UK Natural Environment Research Council (NERC) (grants NE/GE013810/2 and NE/D001471). GOME-2 data was provided by the British Atmospheric Data Centre

GOME-2 formaldehyde retrieval sensitivity

W. Hewson et al.

Title Page

Abstract

Introduction

Conclusions

References

Tables

Figures



Back

Close

Full Screen / Esc

Printer-friendly Version

Interactive Discussion



tesy of EUMETSAT. The authors would also like to acknowledge the continued support of Caroline Fayt at BIRA for assistance with the QDOAS analysis package, Georgina Miles and Richard Siddans at The Rutherford Appleton Laboratory for assistance with cross section convolution, and Marco Vountas at The Institute of Environmental Physics, University of Bremen, for assistance with Ring spectra.

References

- Abbot, D. S., Palmer, P. I., Martin, R. V., Chance, K. V., Jacob, D. J., and Guenther, A.: Seasonal and interannual variability of North American isoprene emissions as determined by formaldehyde column measurements from space, *Geophys. Res. Lett.*, 30, 1886, doi:10.1029/2003GL017336, 2003. 7097
- Aliwell, S. R., Van Roozendaal, M., Johnston, P. V., Richter, A., Wagner, T., Arlander, D. W., Burrows, J. P., Fish, D. J., Jones, R. L., Tørnkqvist, K. K., Lambert, J., Pfeilsticker, K., and Pundt, I.: Analysis for BrO in zenith-sky spectra: an intercomparison exercise for analysis improvement, *J. Geophys. Res.-Atmos.*, 107, 4199, doi:10.1029/2001JD000329, 2002. 7099, 7100, 7106
- Antón, M., Loyola, D., López, M., Vilaplana, J. M., Bañón, M., Zimmer, W., and Serrano, A.: Comparison of GOME-2/MetOp total ozone data with Brewer spectroradiometer data over the Iberian Peninsula, *Ann. Geophys.*, 27, 1377–1386, doi:10.5194/angeo-27-1377-2009, 2009. 7110
- Balis, D., Koukouli, M., Loyola, D., Valks, P., and Hao, N.: Second validation report of GOME-2 total ozone products (OTO/O3, NTO/O3) processed with GDP4.2, Report SAF/O3M/AUTH/GOME-2VAL/RP/02, O3M-SAF, 2008. 7097, 7110
- Barkley, M. P., Palmer, P. I., Kuhn, U., Kesselmeier, J., Chance, K., Kurosu, T. P., Martin, R. V., Helmig, D., and Guenther, A.: Net ecosystem fluxes of isoprene over tropical South America inferred from Global Ozone Monitoring Experiment (GOME) observations of HCHO columns, *J. Geophys. Res.-Atmos.*, 113, D20304, doi:10.1029/2008JD009863, 2008. 7097, 7100, 7113
- Barkley, M. P., Palmer, P. I., De Smedt, I., Karl, T., Guenther, A., and Van Roozendaal, M.: Regulated large-scale annual shutdown of Amazonian isoprene emissions?, *Geophys. Res. Lett.*, 36, L04803, doi:10.1029/2008GL036843, 2009. 7096

GOME-2 formaldehyde retrieval sensitivity

W. Hewson et al.

Title Page

Abstract

Introduction

Conclusions

References

Tables

Figures

◀

▶

◀

▶

Back

Close

Full Screen / Esc

Printer-friendly Version

Interactive Discussion



**GOME-2
formaldehyde
retrieval sensitivity**

W. Hewson et al.

[Title Page](#)[Abstract](#)[Introduction](#)[Conclusions](#)[References](#)[Tables](#)[Figures](#)[◀](#)[▶](#)[◀](#)[▶](#)[Back](#)[Close](#)[Full Screen / Esc](#)[Printer-friendly Version](#)[Interactive Discussion](#)

- Barkley, M. P., Kurosu, T. P., Chance, K., De Smedt, I., Van Roozendael, M., Arneth, A., Hagerberg, D., and Guenther, A.: Assessing sources of uncertainty in formaldehyde air mass factors over tropical South America: Implications for top-down isoprene emission estimates, *J. Geophys. Res.*, 117, D13304, doi:10.1029/2011JD016827, 2012a. 7112
- 5 Barkley, M. P., De Smedt, I., Van Roozendael, M., Kurosu, T. P., Chance, K., Arneth, A., Hagerberg, D., Guenther, A., Paulot, F., Marais, E., and Mao, J.: Top-down isoprene emissions over tropical South America inferred from SCIAMACHY and OMI formaldehyde columns, *J. Geophys. Res.*, in preparation, 2012b. 7112
- 10 Boeke, N. L., Marshall, J. D., Alvarez, S., Chance, K. V., Fried, A., Kurosu, T. P., Rappenglück, B., Richter, D., Walega, J., Weibring, P., and Millet, D. B.: Formaldehyde columns from the Ozone Monitoring Instrument: Urban versus background levels and evaluation using aircraft data and a global model, *J. Geophys. Res.-Atmos.*, 116, D05303, doi:10.1029/2010JD014870, 2011. 7096
- 15 Boersma, K. F., Eskes, H. J., and Brinksma, E. J.: Error analysis for tropospheric NO₂ retrieval from space, *J. Geophys. Res.-Atmos.*, 109, D04311, 1–20, 2004. 7098
- Brauers, T., Bossmeyer, J., Dorn, H.-P., Schlosser, E., Tillmann, R., Wegener, R., and Wahner, A.: Investigation of the formaldehyde differential absorption cross section at high and low spectral resolution in the simulation chamber SAPHIR, *Atmos. Chem. Phys.*, 7, 3579–3586, doi:10.5194/acp-7-3579-2007, 2007. 7108
- 20 Burrows, J. P., Weber, M., Buchwitz, M., Rozanov, V., Ladstätter-Weissenmayer, A., Richter, A., Debeek, R., Hoogen, R., Bramstedt, K., Eichmann, K., Eisinger, M., and Perner, D.: The Global Ozone Monitoring Experiment (GOME): Mission concept and first scientific results, *J. Atmos. Sci.*, 56, 151–175, 1999b. 7097
- 25 Cai, Z., Liu, Y., Liu, X., Chance, K., Nowlan, C. R., Lang, R., Munro, R., and Suleiman, R.: Characterization and correction of Global Ozone Monitoring Experiment 2 ultraviolet measurements and application to ozone profile retrievals, *J. Geophys. Res.*, 117, D07305, doi:10.1029/2011JD017096, 2012. 7104, 7110, 7111
- Caspar, C. and Chance, K.: GOME wavelength calibration using solar and atmospheric spectra, European Space Agency, (Special Publication) ESA SP, 609–612, 1997. 7099, 7125
- 30 Chance, K.: Analysis of BrO measurements from the Global Ozone Monitoring Experiment, *Geophys. Res. Lett.*, 25, 3335–3338, 1998. 7104
- Chance, K.: OMI Trace Gas Algorithms, OMI Algorithm Theoretical Basis Document, Smithsonian Astrophysical Observatory, Cambridge, MA, USA, 2002. 7097, 7103

GOME-2 formaldehyde retrieval sensitivity

W. Hewson et al.

Title Page

Abstract

Introduction

Conclusions

References

Tables

Figures

◀

▶

◀

▶

Back

Close

Full Screen / Esc

Printer-friendly Version

Interactive Discussion



Chance, K., Palmer, P. I., Spurr, R. J. D., Martin, R. V., Kurosu, T. P., and Jacob, D. J.: Satellite observations of formaldehyde over North America from GOME, *Geophys. Res. Lett.*, 27, 3461–3464, 2000. 7097, 7101, 7103

Chance, K., Kurosu, T. P., and Sioris, C. E.: Undersampling correction for array detector-based satellite spectrometers, *Appl. Optics*, 44, 1296–1304, 2005. 7111, 7125

Curci, G., Palmer, P. I., Kurosu, T. P., Chance, K., and Visconti, G.: Estimating European volatile organic compound emissions using satellite observations of formaldehyde from the Ozone Monitoring Instrument, *Atmos. Chem. Phys.*, 10, 11501–11517, doi:10.5194/acp-10-11501-2010, 2010. 7096

De Smedt, I.: Long-Term Global Observations of Tropospheric Formaldehyde Retrieved from Spaceborne Nadir UV Sensors, Ph.D. thesis, Universite Libre De Bruxelles, Laboratoire de Chimie Quantique et Photophysique, Faculté de Sciences Appliquées, 2011. 7099, 7125

De Smedt, I., Müller, J.-F., Stavrou, T., van der A, R., Eskes, H., and Van Roozendael, M.: Twelve years of global observations of formaldehyde in the troposphere using GOME and SCIAMACHY sensors, *Atmos. Chem. Phys.*, 8, 4947–4963, doi:10.5194/acp-8-4947-2008, 2008. 7097, 7100, 7105, 7112, 7113

De Smedt, I., Stavrou, J., Müller, J.-F., Hao, N., Valks, P., Loyola, D., and Van Roozendael, M.: H₂CO Columns Retrieved From GOME-2: First Scientific Results And Progress Towards The Development Of An Operational Product, in: Proceedings of the EUTMETSAT conference, 2009. 7097

De Smedt, I., Stavrou, T., Müller, J., Van Der A, R. J., and Van Roozendael, M.: Trend detection in satellite observations of formaldehyde tropospheric columns, *Geophys. Res. Lett.*, 37, L18808, doi:10.1029/2010GL044245, 2010. 7096

De Smedt, I., Van Roozendael, M., Stavrou, T., Müller, J.-F., Lerot, C., Theys, N., Valks, P., Hao, N., and van der A, R.: Improved retrieval of global tropospheric formaldehyde columns from GOME-2/MetOp-A addressing noise reduction and instrumental degradation issues, *Atmos. Meas. Tech. Discuss.*, 5, 5571–5616, doi:10.5194/amtd-5-5571-2012, 2012. 7097, 7101, 7109

Eisinger, M., Burrows, J. P., Richter, A., and Ladstätter-Weißenmayer, A.: SO₂, OClO, BrO, and other minor trace gases from the Global Ozone Monitoring Experiment (GOME), in: Proceedings of the 3rd ERS-2 Symposium, Florence, Italy, ESA, available at: <http://earth.esa.int/workshops/ers97/papers/eisinger/> (last access: 21 September 2012), 1997. 7097

- EUMETSAT: GOME-2 Product Generation Statement, Tech. Rep. EPS.SYS.SPE.990011, EUMETSAT, 2011. 7101, 7125
- Fayt, C., De Smedt, I., Letocart, V., Merlaud, A., Pinardi, G., and Van Roozendael, M.: QDOAS software user manual, 1.00 Edn., Belgian Institute for Space Aeronomy, Brussels, 2011. 7099
- Fleischmann, O. C., Hartmann, M., Burrows, J. P., and Orphal, J.: New ultraviolet absorption cross-sections of BrO at atmospheric temperatures measured by time-windowing Fourier transform spectroscopy, *J. Photochem. Photobiol. A Chem.*, 168, 117–132, 2004. 7125
- Fu, T., Jacob, D. J., Palmer, P. I., Chance, K., Wang, Y. X., Barletta, B., Blake, D. R., Stanton, J. C., and Pilling, M. J.: Space-based formaldehyde measurements as constraints on volatile organic compound emissions in east and south Asia and implications for ozone, *J. Geophys. Res.-Atmos.*, 112, D06312, doi:10.1029/2006JD007853, 2007. 7097
- Gonzi, S., Palmer, P. I., Barkley, M. P., De Smedt, I., and Van Roozendael, M.: Biomass burning emission estimates inferred from satellite column measurements of HCHO: sensitivity to co-emitted aerosol and injection height, *Geophys. Res. Lett.*, 38, L14807, doi:10.1029/2011GL047890, 2011. 7096
- Herman, J. R. and Celarier, E. A.: Earth surface reflectivity climatology at 340–380 nm from TOMS data, *J. Geophys. Res.*, 102, 28003–28011, doi:10.1029/97JD02074, 1997. 7112
- Kühl, S., Wilms-Grabe, W., Frankenberg, C., Grzegorski, M., Platt, U., and Wagner, T.: Comparison of OCIO nadir measurements from SCIAMACHY and GOME, *Adv. Space Res.*, 37, 2247–2253, 2006. 7101
- Kurosu, T. P., Chance, K., and Sioris, C. E.: Preliminary results for HCHO and BrO from the EOS-aura ozone monitoring instrument, *Proc. SPIE*, 5652, 116–123, 2004. 7097, 7103
- Liu, X., Chance, K., Sioris, C. E., and Kurosu, T. P.: Impact of using different ozone cross sections on ozone profile retrievals from Global Ozone Monitoring Experiment (GOME) ultraviolet measurements, *Atmos. Chem. Phys.*, 7, 3571–3578, doi:10.5194/acp-7-3571-2007, 2007. 7107, 7108
- Loyola, D., Valks, P., Hao, N., Rix, M., and Slijkhuis, S.: Algorithm Theoretical Basis Document for GOME-2 Total Column Products of Ozone, NO₂, tropospheric NO₂, BrO, SO₂, H₂O, HCHO, OCIO and Cloud Properties., Tech. Rep. DLR/GOME-2/ATBD/01, EUMETSAT, 2011a. 7098, 7102
- Loyola, D. G., Koukouli, M. E., Valks, P., Balis, D. S., Hao, N., Van Roozendael, M., Spurr, R. J. D., Zimmer, W., Kiemle, S., Lerot, C., and Lambert, J. C.: The GOME-2 total

AMTD

5, 7095–7139, 2012

**GOME-2
formaldehyde
retrieval sensitivity**

W. Hewson et al.

Title Page

Abstract

Introduction

Conclusions

References

Tables

Figures

◀

▶

◀

▶

Back

Close

Full Screen / Esc

Printer-friendly Version

Interactive Discussion



GOME-2 formaldehyde retrieval sensitivity

W. Hewson et al.

[Title Page](#)
[Abstract](#)
[Introduction](#)
[Conclusions](#)
[References](#)
[Tables](#)
[Figures](#)
[Back](#)
[Close](#)
[Full Screen / Esc](#)
[Printer-friendly Version](#)
[Interactive Discussion](#)


column ozone product: Retrieval algorithm and ground-based validation, *J. Geophys. Res.*, 116, doi:10.1029/2010JD014675, 2011b. 7097, 7110

Malicet, J., Daumont, D., Charbonnier, J., Parisse, C., Chakir, A., and Brion, J.: Ozone UV spectroscopy. II. Absorption cross-sections and temperature dependence, *J. Atmos. Chem.*, 21, 263–273, 1995. 7108, 7125

Marais, E. A., Jacob, D. J., Kurosu, T. P., Chance, K., Murphy, J. G., Reeves, C., Mills, G., Casadio, S., Millet, D. B., Barkley, M. P., Paulot, F., and Mao, J.: Isoprene emissions in Africa inferred from OMI observations of formaldehyde columns, *Atmos. Chem. Phys.*, 12, 6219–6235, doi:10.5194/acp-12-6219-2012, 2012. 7097

Marbach, T., Beirle, S., Penning de Vries, M., Liu, C., and Wagner, T.: Sources and trends of Tropospheric Formaldehyde (HCHO) Sources and trends of Tropospheric Formaldehyde (HCHO) derived from GOME-1 and -2, *Living Planet Symposium, ESA, 2010.* 7102, 7111

Martin, R. V., Chance, K., Jacob, D. J., Kurosu, T. P., Spurr, R. J. D., Bucsela, E., Gleason, J. F., Palmer, P. I., Bey, I., Fiore, A. M., Li, Q., Yantosca, R. M., and Koelemeijer, R. B. A.: An improved retrieval of tropospheric nitrogen dioxide from GOME, *J. Geophys. Res.-Atmos.*, 107, 4437, doi:10.1029/2001JD001027, 2002. 7098, 7112, 7113

Meller, R. and Moortgat, G. K.: Temperature dependence of the absorption cross sections of formaldehyde between 223 and 323 K in the wavelength range 225–375 nm, *J. Geophys. Res.-Atmos.*, 105, 7089–7101, 2000. 7125

Millet, D. B., Jacob, D. J., Turquety, S., Hudman, R. C., Wu, S., Fried, A., Walega, J., Heikes, B. G., Blake, D. R., Singh, H. B., Andersen, B. E., and Clarke, A. D.: Formaldehyde distribution over North America: Implications for satellite retrievals of formaldehyde columns and isoprene emission, *J. Geophys. Res.-Atmos.*, 111, D24S02, doi:10.1029/2005JD006853, 2006. 7097

Millet, D. B., Jacob, D. J., Boersma, K. F., Fu, T., Kurosu, T. P., Chance, K., Heald, C. L., and Guenther, A.: Spatial distribution of isoprene emissions from North America derived from formaldehyde column measurements by the OMI satellite sensor, *J. Geophys. Res.-Atmos.*, 113, D02307, doi:10.1029/2007JD008950, 2008. 7097

Oetjen, H., Wittrock, F., Richter, A., Chipperfield, M. P., Medeke, T., Sheode, N., Sinnhuber, B.-M., Sinnhuber, M., and Burrows, J. P.: Evaluation of stratospheric chlorine chemistry for the Arctic spring 2005 using modelled and measured OCIO column densities, *Atmos. Chem. Phys.*, 11, 689–703, doi:10.5194/acp-11-689-2011, 2011. 7105

GOME-2 formaldehyde retrieval sensitivity

W. Hewson et al.

Title Page

Abstract

Introduction

Conclusions

References

Tables

Figures

◀

▶

◀

▶

Back

Close

Full Screen / Esc

Printer-friendly Version

Interactive Discussion



Palmer, P. I., Jacob, D. J., Chance, K., Martin, R. V., Spurr, R. J. D., Kurosu, T. P., Bey, I., Yantosca, R., Fiore, A., and Li, Q.: Air mass factor formulation for spectroscopic measurements from satellites: application to formaldehyde retrievals from the Global Ozone Monitoring Experiment, *J. Geophys. Res.-Atmos.*, 106, 14539–14550, 2001. 7098, 7112

5 Palmer, P. I., Jacob, D. J., Fiore, A. M., Martin, R. V., Chance, K., and Kurosu, T. P.: Mapping isoprene emissions over North America using formaldehyde column observations from space, *J. Geophys. Res.-Atmos.*, 108, ACH 2–1–2–13, 2003. 7096, 7097, 7099

10 Palmer, P. I., Abbot, D. S., Fu, T., Jacob, D. J., Chance, K., Kurosu, T. P., Guenther, A., Wiedinmyer, C., Stanton, J. C., Pilling, M. J., Pressley, S. N., Lamb, B., and Sumner, A. L.: Quantifying the seasonal and interannual variability of North American isoprene emissions using satellite observations of the formaldehyde column, *J. Geophys. Res.-Atmos.*, 111, D12315, doi:10.1029/2005JD006689, 2006. 7097, 7113

Richter, A. and Burrows, J. P.: Tropospheric NO₂ from GOME measurements, *Adv. Space Res.*, 29, 1673–1683, 2002. 7113

15 Richter, A., Begoin, M., Hilboll, A., and Burrows, J. P.: An improved NO₂ retrieval for the GOME-2 satellite instrument, *Atmos. Meas. Tech.*, 4, 1147–1159, doi:10.5194/amt-4-1147-2011, 2011. 7098

20 Rozanov, A., Rozanov, V., Buchwitz, M., Kokhanovsky, A., and Burrows, J. P.: SCIATRAN 2.0 – a new radiative transfer model for geophysical applications in the 175–2400 nm spectral region, *Adv. Space Res.*, 36, 1015–1019, 2005. 7104, 7125

Shim, C., Wang, Y., Choi, Y., Palmer, P. I., Abbot, D. S., and Chance, K.: Constraining global isoprene emissions with Global Ozone Monitoring Experiment (GOME) formaldehyde column measurements, *J. Geophys. Res.-Atmos.*, 110, 1–14, 2005. 7097

25 Siddans, R., Kerridge, B., and Latter, B.: Analysis of GOME-2 Slit function Measurements, Executive Summary Eumetsat Contract No. EUM/CO/04/1298/RM, Rutherford Appleton Laboratory, 2006. 7099, 7104, 7106, 7125

Spurr, R. J. D., Kurosu, T. P., and Chance, K. V.: A linearized discrete ordinate radiative transfer model for atmospheric remote-sensing retrieval, *J. Quant. Spectrosc. Ra.*, 68, 689–735, 2001. 7112

30 Stavrakou, T., Müller, J., De Smedt, I., Van Roozendaal, M., Van Der Werf, G. R., Giglio, L., and Guenther, A.: Global emissions of non-methane hydrocarbons deduced from SCIAMACHY formaldehyde columns through 2003–2006, *Atmos. Chem. Phys.*, 9, 3663–3679, doi:10.5194/acp-9-3663-2009, 2009a. 7097

**GOME-2
formaldehyde
retrieval sensitivity**

W. Hewson et al.

Title Page

Abstract

Introduction

Conclusions

References

Tables

Figures

◀

▶

◀

▶

Back

Close

Full Screen / Esc

Printer-friendly Version

Interactive Discussion



- Stavrakou, T., Müller, J., De Smedt, I., Van Roozendael, M., Van Der Werf, G. R., Giglio, L., and Guenther, A.: Evaluating the performance of pyrogenic and biogenic emission inventories against one decade of space-based formaldehyde columns, *Atmos. Chem. Phys.*, 9, 1037–1060, doi:10.5194/acp-9-1037-2009, 2009b. 7096
- 5 Theys, N.: Atmospheric Bromine Monoxide: multi-platform observations and model calculations, Ph.D. thesis, Universite Libre De Bruxelles, Laboratoire de Chimie Quantique et Photo-physique, Faculté de Sciences Appliquées, 2010. 7125
- Theys, N., Van Roozendael, M., Hendrick, F., Yang, X., De Smedt, I., Richter, A., Begoin, M., Errera, Q., Johnston, P. V., Kreher, K., and De Mazière, M.: Global observations of tropo-
spheric BrO columns using GOME-2 satellite data, *Atmos. Chem. Phys.*, 11, 1791–1811,
10 doi:10.5194/acp-11-1791-2011, 2011. 7101, 7102
- Thomas, W., Hegels, E., Slijkhuis, S., Spurr, R., and Chance, K.: Detection of biomass burning combustion products in Southeast Asia from backscatter data taken by the GOME spectrom-
eter, *Geophys. Res. Lett.*, 25, 1317–1320, 1998. 7097
- 15 Valks, P., Pinardi, G., Richter, A., Lambert, J.-C., Hao, N., Loyola, D., Van Roozendael, M., and Emmadi, S.: Operational total and tropospheric NO₂ column retrieval for GOME-2, *Atmos. Meas. Tech.*, 4, 1491–1514, doi:10.5194/amt-4-1491-2011, 2011. 7098, 7111
- Vandaele, A. C., Hermans, C., Simon, P. C., Carleer, M., Colin, R., Fally, S., Mérienne, M. F., Jenouvrier, A., and Coquart, B.: Measurements of the NO₂ absorption cross-section from
20 42 000 cm⁻¹ to 10 000 cm⁻¹ (238–1000 nm) at 220 K and 294 K, *J. Quant. Spectrosc. Ra.*, 59, 171–184, 1998. 7125
- Van Geffen, J. H. G. M. and Van Oss, R. F.: Wavelength calibration of spectra measured by the global ozone monitoring experiment by use of a high-resolution reference spectrum, *Appl. Optics*, 42, 2739–2753, 2003. 7099
- 25 Van Roozendael, M., Soebijanta, V., Fayt, C., and Lambert, J.-C.: Investigation of DOAS issues affecting the accuracy of the GDP version 3.0 total ozone product, Tech. rep., Space Aeronomy Institute of Belgium, Brussels, 2002. 7097
- Vountas, M., Rozanov, V. V., and Burrows, J. P.: Ring effect: Impact of rotational Raman scattering on radiative transfer in earth's atmosphere, *J. Quant. Spectrosc. Ra.*, 60, 943–961, 1998.
30 7104, 7125
- Vrekoussis, M., Wittrock, F., Richter, A., and Burrows, J. P.: GOME-2 observations of oxygenated VOCs: what can we learn from the ratio glyoxal to formaldehyde on a global scale?, *Atmos. Chem. Phys.*, 10, 10145–10160, doi:10.5194/acp-10-10145-2010, 2010. 7097

Wang, P., Stammes, P., van der A, R., Pinardi, G., and van Roozendael, M.: FRESCO+: an improved O₂ A-band cloud retrieval algorithm for tropospheric trace gas retrievals, Atmos. Chem. Phys., 8, 6565–6576, doi:10.5194/acp-8-6565-2008, 2008. 7112

5 Wittrock, F.: The retrieval of oxygenated volatile organic compounds by remote sensing techniques, Ph.D. thesis, Universität Bremen, Bremen, 2006. 7097

Wittrock, F., Richter, A., Ladstätter-Weißmayer, A., and Burrows, J. P.: Global observations of formaldehyde, in: European Space Agency, (Special Publication) ESA SP, 1358–1362, 2000. 7100, 7103, 7109

AMTD

5, 7095–7139, 2012

**GOME-2
formaldehyde
retrieval sensitivity**W. Hewson et al.

[Title Page](#)[Abstract](#)[Introduction](#)[Conclusions](#)[References](#)[Tables](#)[Figures](#)[⏪](#)[⏩](#)[◀](#)[▶](#)[Back](#)[Close](#)[Full Screen / Esc](#)[Printer-friendly Version](#)[Interactive Discussion](#)

GOME-2 formaldehyde retrieval sensitivity

W. Hewson et al.

[Title Page](#)
[Abstract](#)
[Introduction](#)
[Conclusions](#)
[References](#)
[Tables](#)
[Figures](#)
[Back](#)
[Close](#)
[Full Screen / Esc](#)
[Printer-friendly Version](#)
[Interactive Discussion](#)


Table 1. Default retrieval settings used in the sensitivity analysis, based on De Smedt (2011). Differences to the original retrieval are the inclusion of an undersampling cross section, and exclusion of an OCIO fit.

Parameter	Setting
Fit window	BrO 328.5–359 nm (Theys, 2010) HCHO 328.5–346 nm (De Smedt, 2011)
Polynomial	5th order
Cross sections	BrO (223 K) (Fleischmann et al., 2004) HCHO (298 K) (Meller and Moortgat, 2000) NO ₂ (220 K) (Vandaele et al., 1998) O ₃ (228 and 243 K) (Malicet et al., 1995) (I ₀ corrected to 0.8 × 10 ¹⁹)
Linear offset	1st order
Ring	Vountas et al. (1998) and Rozanov et al. (2005)
Undersampling	Chance et al. (2005)
Scan bias correction	Eta and zeta polarisation vectors (EUMETSAT, 2011)
Slit function	Siddans et al. (2006)
Solar reference	GOME-2 daily solar mean reference
I ₀ calibration	Caspar and Chance (1997)

GOME-2 formaldehyde retrieval sensitivity

W. Hewson et al.

Table 2. Parameter effects on mean HCHO slant columns, ± 1 standard deviation, and mean RMS residuals (RMS) over the entire globe, Amazon, Southeast US, and remote Pacific Ocean regions (as defined in Fig. 1). Slant column units are $\times 10^{16}$ molecules cm^{-2} and residual root mean-square (RMS) values are $\times 10^{-4}$.

Setting	Global			Amazon (AMA)			Southeast US (SEUS)			Pacific Ocean (PAC)		
	Mean	$\pm 1\sigma$	RMS	Mean	$\pm 1\sigma$	RMS	Mean	$\pm 1\sigma$	RMS	Mean	$\pm 1\sigma$	RMS
Reference retrieval	-0.30	0.57	8.87	1.01	0.33	8.37	1.14	0.32	7.96	-0.35	0.15	7.89
Spectral range												
BrO window												
1a. 332–359 nm	-0.24	0.57	8.87	1.01	0.34	8.38	1.21	0.32	7.95	-0.29	0.16	7.88
1b. 332–359 nm (+ OCIO)	-0.15	0.56	8.85	1.09	0.35	8.36	1.27	0.32	7.94	-0.21	0.16	7.87
1c. Pre-fit BrO and O ₃	-0.28	0.58	8.90	1.03	0.33	8.40	1.19	0.32	7.95	-0.34	0.15	7.90
HCHO window												
2a. 325.5–350 nm	0.27	0.61	9.79	1.37	0.29	9.11	1.64	0.31	8.49	0.07	0.14	8.57
2b. 332–350 nm	-0.38	0.59	9.42	0.99	0.37	8.94	1.09	0.33	8.43	-0.41	0.16	8.42
2c. 337.5–359 nm (GOME-1)	-1.48	0.75	10.82	0.02	0.47	10.31	0.03	0.38	9.81	-1.50	0.17	9.72
2d. 327.5–356.6 nm (OMI)	-0.35	0.63	9.93	0.75	0.31	9.28	0.98	0.32	8.70	-0.56	0.13	8.66
Absorber effects												
3a. O ₄	-0.16	0.54	8.84	1.12	0.36	8.31	1.20	0.32	7.94	-0.22	0.16	7.85
3b. O ₄ (GOME-1 window)	-1.38	0.77	10.73	0.10	0.49	10.25	0.08	0.38	9.78	-1.41	0.18	9.67
3c. O ₄ (3rd order poly)	0.64	0.55	8.89	1.81	0.33	8.36	2.01	0.33	7.94	0.51	0.14	7.85
3d. OCIO	-0.40	0.59	8.83	0.92	0.35	8.34	1.06	0.34	7.95	-0.51	0.16	7.84
3e. No wav. calibration	-1.11	0.64	9.18	0.33	0.33	8.58	0.38	0.32	8.25	-1.03	0.15	8.08
3f. I ₀ correct all abs.	-0.30	0.55	8.83	1.02	0.32	8.33	1.10	0.32	7.92	-0.32	0.15	7.85
Polynomial degree												
4a. 4th order polynomial	0.01	0.61	8.97	1.25	0.31	8.44	1.45	0.33	8.03	-0.14	0.14	7.95
4b. 3rd order polynomial	-0.35	0.72	9.20	0.89	0.30	8.63	1.23	0.34	8.10	-0.45	0.15	8.12
Instrument corrections												
5a. No scan bias correction	0.10	0.57	8.81	1.34	0.32	8.32	1.48	0.32	7.92	0.00	0.14	7.83
5b. No under-sampling	-0.17	0.56	8.98	1.05	0.33	8.41	1.29	0.33	8.04	-0.31	0.16	7.93
5c. No linear offset	-1.34	0.62	9.48	0.22	0.34	8.78	0.22	0.33	8.48	-1.59	0.14	8.77
5d. 0 order offset correction	-1.13	0.62	9.28	0.38	0.34	8.65	0.42	0.33	8.32	-1.27	0.14	8.38
5e. 2nd order offset correction	-0.24	0.56	8.83	1.07	0.33	8.32	1.19	0.32	7.93	-0.30	0.15	7.87
5f. 1/I ₀ offset correction	-1.15	0.61	9.27	0.35	0.34	8.65	0.38	0.33	8.32	-1.33	0.14	8.39

Title Page

Abstract

Introduction

Conclusions

References

Tables

Figures

◀

▶

◀

▶

Back

Close

Full Screen / Esc

Printer-friendly Version

Interactive Discussion



**GOME-2
formaldehyde
retrieval sensitivity**

W. Hewson et al.

Title Page

Abstract

Introduction

Conclusions

References

Tables

Figures

◀

▶

◀

▶

Back

Close

Full Screen / Esc

Printer-friendly Version

Interactive Discussion



Table 3. Monthly mean HCHO vertical columns for August 2007 (units of $\times 10^{16}$ molecules cm^{-2}) derived from usage of unique directional swath components for the reference sector correction, taking the reference retrieval as source data.

Scans	Global	AMA	SEUS	PAC
All	0.49	1.62	2.02	0.31
Back	0.45	1.58	1.98	0.28
Front	0.49	1.63	2.02	0.31
Centre	0.30	1.36	1.73	0.12
East	0.54	1.83	2.23	0.46
West	0.30	1.36	1.73	0.12

GOME-2 formaldehyde retrieval sensitivity

W. Hewson et al.

Table 4. Summary of mean vertical columns (units of $\times 10^{16}$ molecules cm^{-2}) for selected tests, the range of which are in sharp contrast to the variability found with their the SC precursors (a full table of results is available from the authors).

Fit window (nm)	Global		AMA		SEUS		PAC	
	Mean	$\pm 1\sigma$	Mean	$\pm 1\sigma$	Mean	$\pm 1\sigma$	Mean	$\pm 1\sigma$
Reference retrieval	0.49	0.43	1.62	0.35	2.02	0.44	0.31	0.11
Spectral range								
BrO window								
1a. 332–359	0.50	0.43	1.57	0.36	2.03	0.44	0.32	0.11
1b. 332–359 (+ OCIO)	0.48	0.42	1.56	0.36	1.98	0.44	0.31	0.12
HCHO window								
2a. 325.5–350	0.57	0.48	1.54	0.31	2.05	0.44	0.30	0.10
2b. 332–350	0.49	0.44	1.70	0.40	2.07	0.46	0.33	0.11
2c. 337.5–359	0.39	0.56	1.76	0.49	1.98	0.52	0.28	0.13
2d. 327.5–356.6	0.51	0.48	1.52	0.32	1.89	0.45	0.27	0.09
Absorber effects								
3a. O ₄	0.41	0.41	1.57	0.37	1.84	0.43	0.28	0.11
3c. OCIO	0.51	0.47	1.71	0.37	2.12	0.48	0.33	0.11
3e. I ₀ correct all abs.	0.49	0.42	1.61	0.34	2.00	0.44	0.32	0.11
Polynomial degree								
4a. 4th order polynomial	0.55	0.47	1.65	0.32	2.06	0.46	0.31	0.10
4b. 3rd order polynomial	0.58	0.51	1.62	0.32	2.11	0.47	0.31	0.11
Instrument corrections								
5a. No scan bias correction	0.52	0.43	1.61	0.34	1.98	0.44	0.32	0.10
5b. No under-sampling	0.52	0.44	1.64	0.35	2.07	0.45	0.32	0.11

Title Page

Abstract

Introduction

Conclusions

References

Tables

Figures

◀

▶

◀

▶

Back

Close

Full Screen / Esc

Printer-friendly Version

Interactive Discussion



GOME-2 formaldehyde retrieval sensitivity

W. Hewson et al.

Table 5. Summary of the reference sector correction on the retrieved HCHO vertical columns relative to the default reference retrieval (i.e. ΔVC). The slant column differences (ΔSC) from each test are also shown for comparison. Differences are in %.

Test	Global		AMA		SEUS		PAC	
	ΔSC	ΔVC						
Spectral range (nm)								
BrO window								
1a. 332–359	21	1	0	-3	6	1	17	2
1b. 332–359 (+ OCIO)	49	-2	8	-4	12	-2	40	-0
HCHO window								
2a. 325.5–350	190	16	35	-5	44	2	121	-2
2b. 332–350	-27	-1	-2	5	-4	3	-16	7
2c. 337.5–359	-390	-21	-98	8	-97	-2	-328	-9
2d. 327.5–356.6	-17	3	-26	-6	-14	-6	-60	-14
Absorber effects								
3a. O ₄	-46	17	11	3	6	9	-38	8
3c. OCIO	32	-4	-9	-6	-7	-5	45	-5
3e. I ₀ correct all abs.	0	2	1	1	-3	1	-8	-2
Polynomial degree								
4a. 4th order polynomial	-105	-11	23	-2	27	-2	-60	0
4b. 3rd order polynomial	16	-17	-11	0	8	-5	28	0
Instrument corrections								
5a. No scan bias correction	133	5	32	1	30	2	99	3
5b. No under-sampling	45	5	4	1	14	3	13	5

Title Page

Abstract

Introduction

Conclusions

References

Tables

Figures

◀

▶

◀

▶

Back

Close

Full Screen / Esc

Printer-friendly Version

Interactive Discussion



**GOME-2
formaldehyde
retrieval sensitivity**

W. Hewson et al.

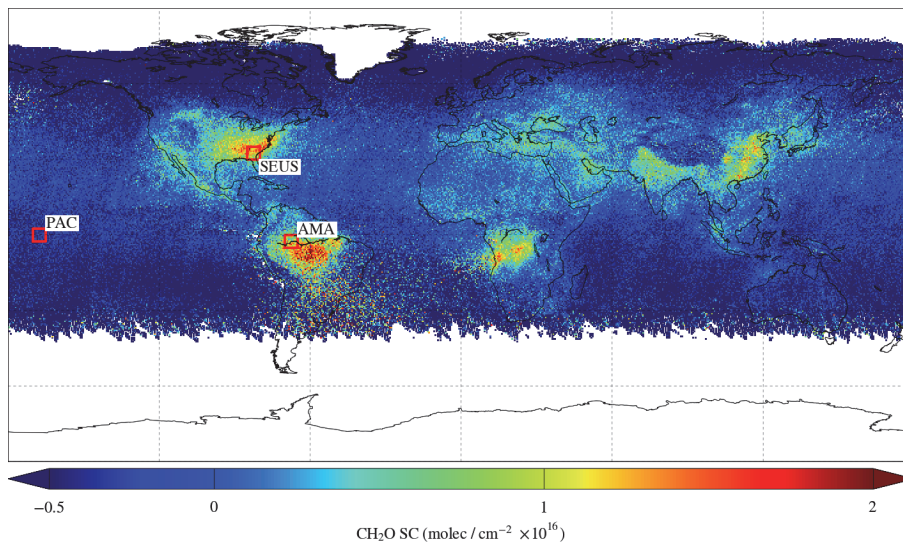


Fig. 1. Monthly mean HCHO slant columns for August 2007 retrieved using the default algorithm settings (Table 1). The data are averaged onto a $0.5^\circ \times 0.5^\circ$ grid excluding observations with cloud fraction > 0.4 and solar zenith angles $> 60^\circ$.

[Title Page](#)[Abstract](#)[Introduction](#)[Conclusions](#)[References](#)[Tables](#)[Figures](#)[◀](#)[▶](#)[◀](#)[▶](#)[Back](#)[Close](#)[Full Screen / Esc](#)[Printer-friendly Version](#)[Interactive Discussion](#)

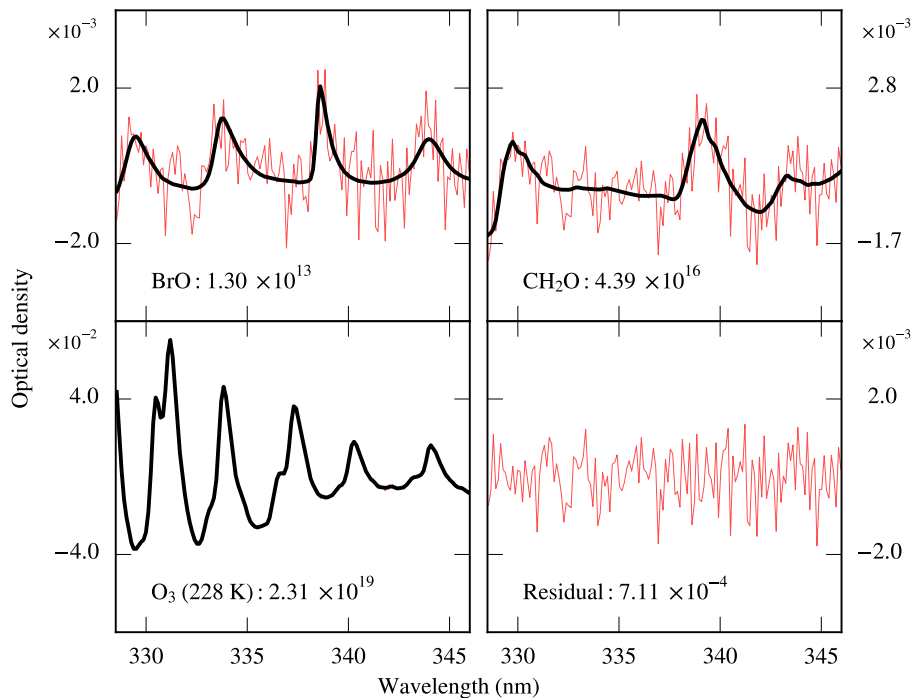


Fig. 2. Example HCHO fit using the reference retrieval settings for an enhanced HCHO plume over the South East USA on the 9 August 2007 (scan 3107, orbit 4176, SZA 28.8°). NO₂, Ring, under-sampling, polynomial fit, and linear offset are omitted from the plot, but included in the fit; slant column units are in molecules cm⁻².

**GOME-2
formaldehyde
retrieval sensitivity**

W. Hewson et al.

Title Page

Abstract

Introduction

Conclusions

References

Tables

Figures

◀

▶

◀

▶

Back

Close

Full Screen / Esc

Printer-friendly Version

Interactive Discussion



GOME-2 formaldehyde retrieval sensitivity

W. Hewson et al.

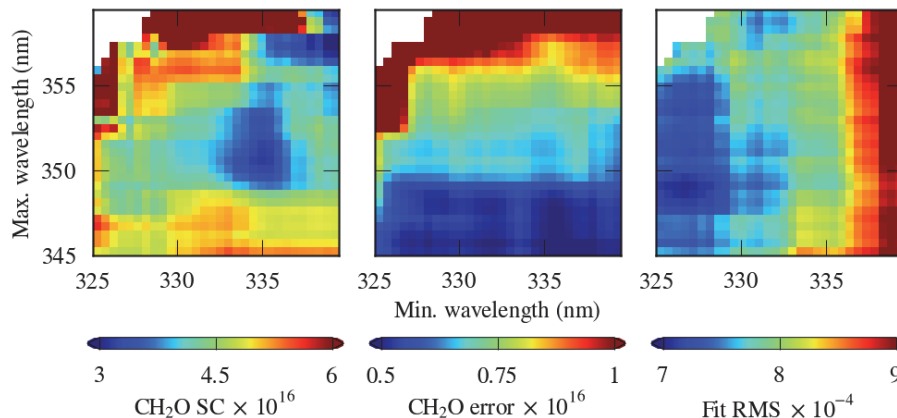


Fig. 3. This surface plot (scan number 3107, orbit 4176) takes the reference retrieval and adjusts the upper and lower limits of the HCHO fit window in 0.5 nm increments, revealing the large variations in slant column and concurrent errors to be found within the HCHO fitting window. Note areas of low slant column error and fit RMS coincide well with the baseline retrieval window of 328.5–346 nm on the x and y axis, respectively. Differences between HCHO error and fit residuals are suggested to be attributed to variation in the error covariance matrix as the fit boundary is adjusted (M. Van Roozendael, personal communication, 2012).

Title Page

Abstract

Introduction

Conclusions

References

Tables

Figures

◀

▶

◀

▶

Back

Close

Full Screen / Esc

Printer-friendly Version

Interactive Discussion



**GOME-2
formaldehyde
retrieval sensitivity**

W. Hewson et al.

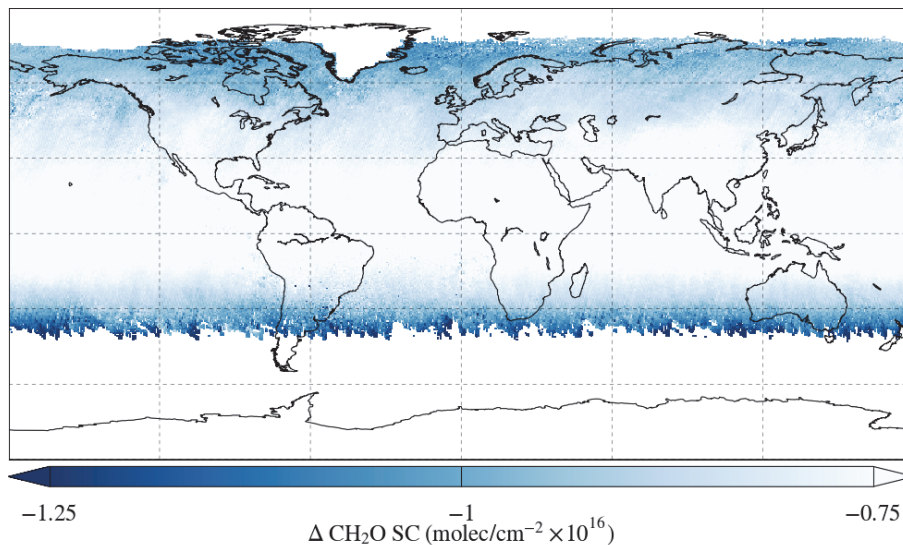


Fig. 4. Difference plot on monthly mean for test 3d, excluding wavelength calibration. Dark fringes at the latitudinal extremes of the retrievals indicate HCHO slant columns are strongly depressed in these regions, primarily as a function of increased O_3 interference.

[Title Page](#)[Abstract](#)[Introduction](#)[Conclusions](#)[References](#)[Tables](#)[Figures](#)[◀](#)[▶](#)[◀](#)[▶](#)[Back](#)[Close](#)[Full Screen / Esc](#)[Printer-friendly Version](#)[Interactive Discussion](#)

GOME-2 formaldehyde retrieval sensitivity

W. Hewson et al.

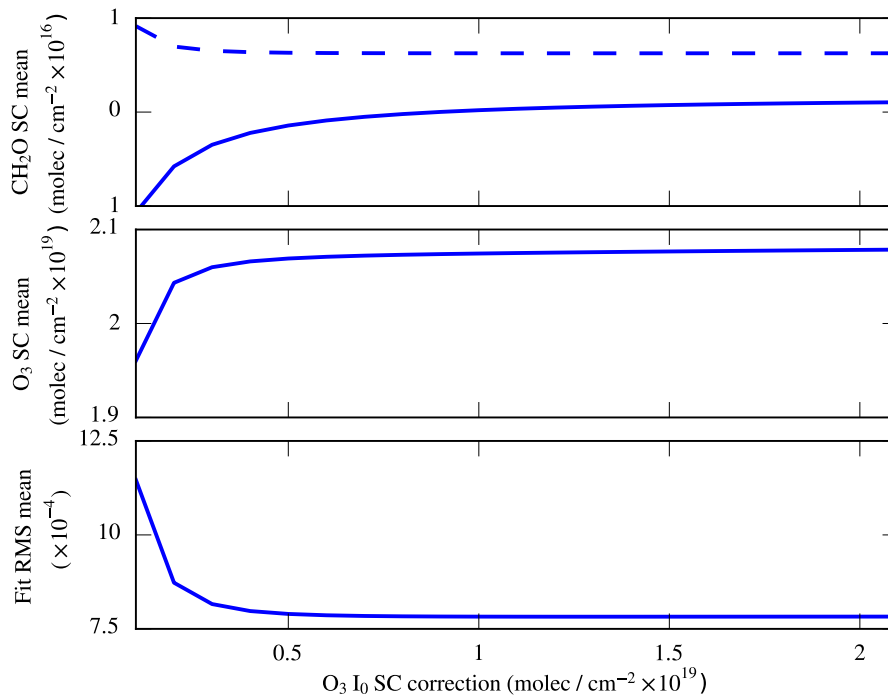


Fig. 5. I_0 correction range test showing mean values for orbit 4176, with the O_3 column add back adjusted at 0.1×10^{19} molecules cm^{-2} intervals along the x axis (the reference retrieval applies an add back value of 0.8×10^{19} molecules cm^{-2}). Dashed line indicates mean HCHO slant column error.

Title Page

Abstract

Introduction

Conclusions

References

Tables

Figures

◀

▶

◀

▶

Back

Close

Full Screen / Esc

Printer-friendly Version

Interactive Discussion



GOME-2 formaldehyde retrieval sensitivity

W. Hewson et al.

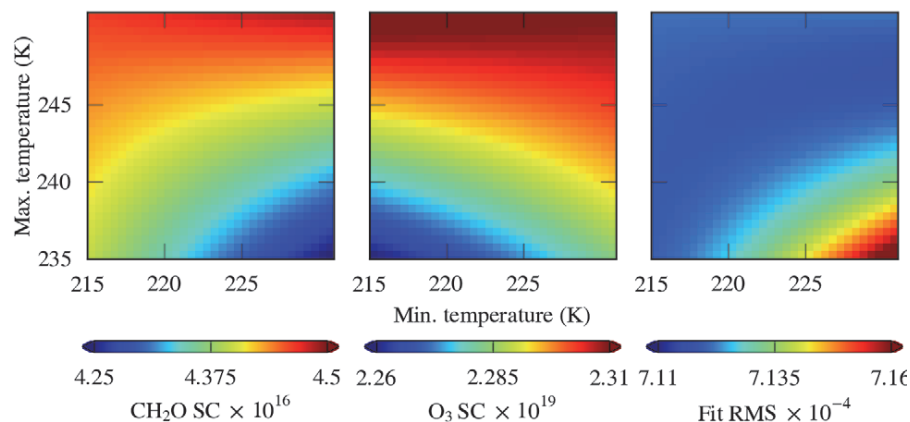


Fig. 6. This surface plot (scan number 3107, orbit 4176) takes the reference retrieval and adjusts the low and high temperatures (x and y axes, respectively) of the orthogonalised O₃ absorption spectra in 0.5K increments. A linear gradient is seen for slant columns (molecules cm⁻²) and fit residuals. Whilst the range of fit residual variation is not large, the retrieved HCHO slant column displays a non-negligible range of values.

Title Page

Abstract

Introduction

Conclusions

References

Tables

Figures

◀

▶

◀

▶

Back

Close

Full Screen / Esc

Printer-friendly Version

Interactive Discussion



**GOME-2
formaldehyde
retrieval sensitivity**

W. Hewson et al.

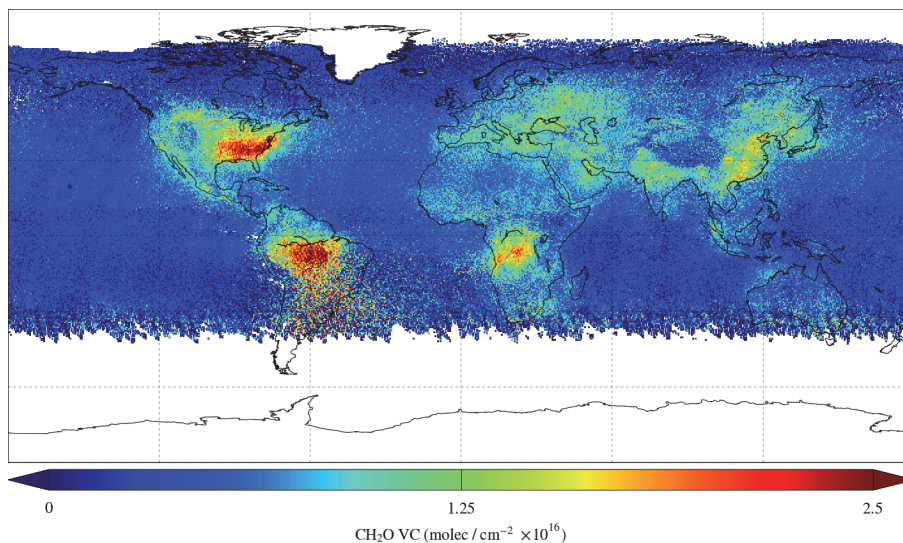


Fig. 7. Monthly mean HCHO vertical columns for August 2007 retrieved using the default algorithm settings (Table 1), after the application of the reference sector correction (see Sect. 4.2). Data are averaged onto a $0.5^\circ \times 0.5^\circ$ grid excluding observations with cloud fraction > 0.4 and SZA $> 60^\circ$.

Title Page

Abstract

Introduction

Conclusions

References

Tables

Figures

◀

▶

◀

▶

Back

Close

Full Screen / Esc

Printer-friendly Version

Interactive Discussion



GOME-2 formaldehyde retrieval sensitivity

W. Hewson et al.

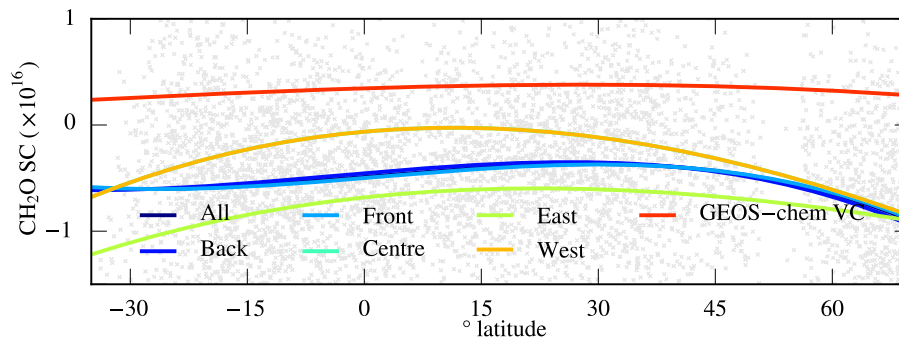


Fig. 8. Reference sector correction for the 9 August 2007. Grey markers indicate retrieved slant column values in the reference strip from which we model our subtractive polynomial. Solid lines represent the polynomial taken from these values according to scan position. Note large differences between east and west swath corrections, illustrating bias present in retrievals according to swath position. “All” is obscured by “Back” and “Front”, whilst “Centre” is obscured by “West”.

Title Page

Abstract

Introduction

Conclusions

References

Tables

Figures

◀

▶

◀

▶

Back

Close

Full Screen / Esc

Printer-friendly Version

Interactive Discussion



GOME-2 formaldehyde retrieval sensitivity

W. Hewson et al.

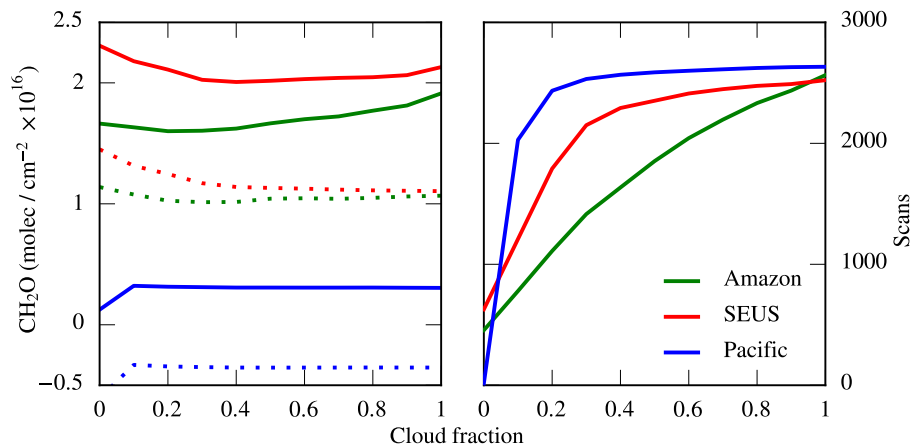


Fig. 9. Removing the cloud fraction threshold from our reference retrieval shows the wide range of HCHO slant columns (left hand plot, dotted lines), vertical columns (left hand plot, solid lines), and scan counts (right hand plot) taken into monthly means for the three detailed study sites. A cloud fraction (CF) of 1 indicates all scans are taken into account. Over the AMA study site, above cloud vertical column enhancements are evident when relaxing the CF threshold above > 0.4 .

Title Page

Abstract

Introduction

Conclusions

References

Tables

Figures

◀

▶

◀

▶

Back

Close

Full Screen / Esc

Printer-friendly Version

Interactive Discussion



**GOME-2
formaldehyde
retrieval sensitivity**

W. Hewson et al.

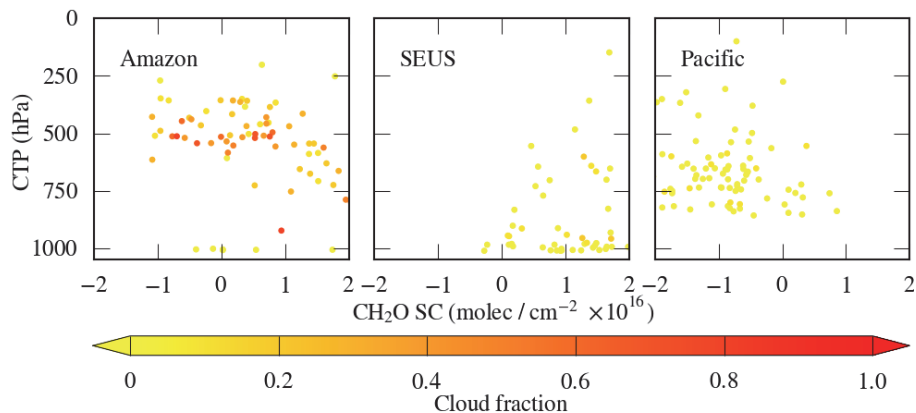


Fig. 10. CH_2O SC against cloud top pressure (CTP), with cloud fractions from 0–1.0 denoted by colour, for the three study sites on the 9 August 2007. The Amazon site shows the large amounts of high CF scans expected in the region due to the regional climate, all of which are in the 300–600 hPa region, whilst the South Eastern US and Pacific Ocean regions display no clear correlation between CF and CTP.

Title Page

Abstract

Introduction

Conclusions

References

Tables

Figures

◀

▶

◀

▶

Back

Close

Full Screen / Esc

Printer-friendly Version

Interactive Discussion

